Aggregate Interference Analysis for Interweave Cognitive Networks

S. Kusaladharma, P. Herath and C. Tellambura, *Fellow*, *IEEE*
Department of Electrical and Computer Engineering
University of Alberta, Edmonton, Alberta T6G 2V4, Canada
Email: {kusaladh,prasanna}@ualberta.ca and chintha@ece.ualberta.ca

***Abstract*—This paper investigates the aggregate interference from interweave cognitive secondary nodes spatially distributed in a finite Poisson field. These secondary nodes sense an out-of-band beacon to initiate their transmissions, which can be concurrent with those of the primary system if a sensing error is made. The resulting aggregate interference is analyzed in this paper. For this purpose, general Nakagami-m fading and path-loss are assumed for all relevant channels. Moreover, we incorporate random secondary node transmit powers with any probability distribution. The analysis includes the exact moment generating function (MGF) of the aggregate interference along with the exact outage probability of the primary system. Furthermore, we develop a simple MGF approximation which is valid for severely fading channels and for lower beacon reception threshold to beacon transmit power ratios. Finally, we show that a lower fading severity significantly improves the diversity order of the PR due to more accurate spectrum sensing by the secondary nodes.**

I. Introduction

Secondary nodes of interweave cognitive radio (CR) networks sense unused frequency chunks [1] by processing a beacon signal (pilot channel) transmitted from either the primary transmitter or the primary receiver (PR) [2]. If the beacon is detected, the secondary nodes will cease transmission within that particular frequency slot. If not, they are allowed to use it.

Consequently, if secondary nodes misdetect the beacon signal, their concurrent transmissions with those of the primary system interfere with and degrade the performance of the PR. Beacon misdetection may be caused by wireless signals undergoing path-loss, fading, and shadowing. The aggregate interference due to beacon misdetection also depends on the random secondary node distribution (numbers and locations). Statistical characterization of the aggregate interference helps in the design of system parameters (suitable node densities, geographical areas for deployment etc.), power control schemes, and sensing schemes in practical CR standards such as IEEE 802.22 [3]. To this end, this paper analyzes the aggregate interference, and PR performance for interweave CR networks.

A. Previous Research

Several recent works have addressed the issue of the aggregate interference with or without the use of beacons. Bounds for the aggregate interference and outage probability are derived in [4] along with Poisson-cluster based approximations for interference among secondary nodes, while an approximation for the aggregate interference based on a normal and log-normal sum is developed in [5]. Reference [6] analyzes the CR coverage performance, while statistics and bounds for the aggregate interference are analyzed in [7].

Several other works incorporate spectrum sensing with beacon misdetection into their analysis. Reference [2] analyzes the resulting capacity-outage due to beacon misdetection in Rayleigh and Nakagami-m fading. In [8], aggregate interference statistics are modeled incorporating spectrum sensing and channel parameters, leading to the characteristic function and cumulants. Moreover, in [9], the aggregate interference and outage was analyzed for Rayleigh fading channels.

B. Motivation and Contribution

In all the previous works analyzing aggregate interference from interweave nodes employing beacon detection, at least one of the following restrictive assumptions is made:

i The number of interferers is constant,
ii Each secondary node transmits with a constant power,
iii Channel gains due to small-scale fading are exponential (Rayleigh fading).

However, in modern wireless networks, since both the location and number of nodes in a given area is time varying, node locations should be modeled via a spatial point process. To remedy this, the Poisson Point Process (PPP) [10] has extensively been used [8], [11]–[13]. Moreover, in practical communication networks (mobile, sensor, personal area, and ad-hoc networks etc.), nodes may transmit at a power level that depends on many factors such as the distance between the transmitter and the receiver, maximum allowed transmit power, and type of the device. Furthermore, the degree of fading in radio channels will vary depending on the environment.

These factors suggest that a more general analysis which eliminates these assumptions is desirable. To this end, we develop a generalized analysis of: (i) the moment generating function (MGF) of the aggregate interference, and (ii) the outage probability of the PR. The MGF is an important measure because it completely describes a probability distribution and because further statistics such as moments are easily obtained from it.

In order to model the random locations of the secondary nodes, a homogeneous PPP is used. We will use independent thinning and mapping for PPPs (explained in the next section) in order to simplify our analysis. To accommodate variations of secondary node transmit power, random transmit powers with a given statistical distribution for the secondary nodes are considered. Furthermore, the Nakagami-m fading model

978-1-4799-4449-1/14/$31.00 ©2014 IEEE

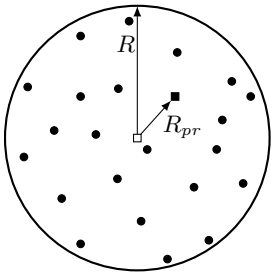

Fig. 1: Sytem model. The secondary nodes (dots) are located in a circular area of radius R. R_{pr} is the primary transmitter (black square) to primary receiver (white square) distance.

provides a closer match to experimental data and represents a wider range of fading severities [14]. As such, we will be using it for our analysis. Moreover, [2] used an approximation for the beacon misdetection probability for a constant number of interferers. We will investigate the accuracy of this approximation for PPPs under varying system/channel parameters.

Notations: $\Gamma(x,a) = \int_a^\infty t^{x-1}e^{-t}dt$, $\Gamma(x) = \Gamma(x,0)$, and ${}_2\mathcal{F}_1(,;;)$ is the Gauss' Hypergeometric function [15]. $\Pr[A]$ is the probability of event A, $f_X(\cdot)$ is the probability density function (PDF), $F_X(\cdot)$ is the cumulative distribution function (CDF), $M_X(\cdot)$ is the MGF, $X^{(\mu)}(s)$ is the μ-th derivative of X with respect to s, and $E_X[\cdot]$ denotes the expectation over random variable X. The PPP is defined in [10, p. 11].

II. System model

This section introduces the spatial and signal models. We will consider a circular region of secondary nodes for this analysis (Fig. 1). Without loss of generality, the PR is taken to be located at the center, and the primary transmitter is located at a distance R_{pr} from the PR. The radius of the region is taken as R. A finite region provides generality for the analysis, and an infinite region would be a special case when $R \to \infty$. In this paper, we will model the spatial distribution of secondary nodes via a homogeneous PPP (the node density is independent of the spatial location). Two special characteristics of PPPs, namely independent thinning and mapping will be used to aid our analysis. Independent thinning refers to coloring points of a PPP Π with intensity μ independently; where the probability of a point receiving the t-th color is p_t, and obtaining the set of points with the t-th color Π_t which is a PPP with intensity $\mu_t = p_t\mu$ [10]. As a practical example, some secondary nodes may be active and others not. Thinning would remove the inactive nodes. Mapping refers to the transformation of a PPP of a_1 dimensions to another equivalent PPP with a_2 dimensions where $a_1 > a_2$ [10].

According to the PPP distribution, the probability of having n secondary nodes within a certain area A is given by [16],

$$P(n) = \frac{(\lambda A)^n}{n!}e^{-\lambda A}, \quad n = 0, 1, 2\ldots, \tag{1}$$

where λ is the intensity/ node density. As a homogeneous PPP is considered, λ does not depend on the location. Moreover, we will assume that all secondary nodes are opportunistically trying to access the spectrum. Although it appears that this assumption provides the worst-case scenario with respect to the interference experienced at the PR, no loss of generality occurs. This is due to the probability that a secondary node requiring to transmit (κ) being independent from other nodes. Independent thinning can be performed to thin the PPP with intensity λ to an equivalent PPP with intensity $\kappa\lambda$ using the Coloring theorem for PPPs [10]. As such, we can incorporate the activity factor into the secondary node intensity directly. Furthermore, the higher layer protocols and network operations are out of scope for this paper.

In an interweave network, the secondary nodes sense the spectrum and transmits only when the primary signals are absent. To achieve this, the presence of an out-of-band beacon transmission originating from the PR is detected. The secondary nodes transmit either when the beacon is absent or when the beacon is not detected. Thus, interference is caused to the PR when a secondary node transmission takes place after beacon misdetection. The primary signals, secondary signals, and the beacon signals all undergo path-loss and Nakagami-m fading.

We will use the simplified path-loss model [14], where the received power P at a distance of r from the transmitter is given as $P = P_T r^{-\alpha}$. P_T is given as $P_T = P_0 r_0^\alpha$, where P_0 is the received power at a distance r_0 from the transmitter. The Nakagami-m channel power gain for the i-th secondary node follows a gamma distribution which is given by [17],

$$f_{|h_i|^2}(x) = \frac{m^m}{\Gamma(m)}x^{m-1}e^{-mx}, 0 \le x < \infty, 0.5 < m < \infty, \tag{2}$$

where the Nakagami parameter m is a measure of fading severity, and larger m indicates milder fading ($m = \infty$ equates to no fading). Since the gamma approximation is also feasible for composite shadowing and Nakagami-m fading [18] , the following analysis could be easily amended to incorporate shadowing.

III. Interference Analysis

This section will derive the MGF of the aggregate interference, which leads to the derivation of the outage performance. We will use the principle of mapping described before in order to simplify the analysis.

The aggregate interference (I) can be written as $I = \sum_{i=1}^N I_i$, where the number of transmitting secondary nodes is given by N, and the interference from the i-th transmitting secondary node is given by I_i. I_i is written as $I_i = P_{CR}|h_i|^2 r^{-\alpha}$, where $|h_i|^2$ is the channel gain, r is the distance from the secondary node to the PR, α is the path-loss exponent, and P_{CR} is the power level of the secondary node.

A. The mapping procedure

We are considering a homogeneous PPP with density λ in an annular area with radius R. This 2-D homogeneous PPP can be mapped to a equivalent (in terms of the distance distribution) 1-D non-homogeneous PPP with intensity function λ_1 [10]

where

$$\lambda_1 = \int_0^{2\pi} \lambda r d\theta = 2\pi\lambda r, 0 < r < R. \quad (3)$$

However, only the secondary nodes misdetecting the beacon transmission will be causing interference. Let β be the probability of beacon misdetection for any given secondary node. β is dependent on factors including the path-loss exponent, secondary node-PR distance, and fading. If P_b is the power level of the beacon transmission, P_{T_b} is the power threshold required by the secondary nodes for correct reception of the beacon, and $|g_i|^2$ is the gain of the beacon channel, β is obtained as

$$\beta = \Pr\left[P_b|g_i|^2 r^{-\alpha} < P_{T_b}\right] = \sum_{k=0}^{\infty} \frac{(-1)^k}{k!} \frac{(m\frac{P_{T_b}}{P_b} r^{\alpha})^{m+k}}{(m+k)\Gamma(m)} \quad (4)$$

When $\frac{P_{T_b}}{P_b}$ and m are low, we can approximate β with only the first term as $\beta \approx \frac{(m\frac{P_{T_b}}{P_b} r^{\alpha})^m}{m\Gamma(m)}$. However, we will conduct the analysis using the exact result (4), and will elaborate on the accuracy of this approximation within Section V.

For any secondary node, although β depends on r, it doesn't depend on the locations of other nodes. Therefore, using the Coloring theorem [10], independent thinning can be performed on the 1-D PPP obtained earlier. Thus, the resulting density of the thinned 1-D PPP ($\bar{\lambda}$) is given by $\bar{\lambda} = \beta\lambda_1$ which equates to

$$\bar{\lambda} = 2\pi\lambda \sum_{k=0}^{\infty} \frac{(-1)^k}{k!} \frac{(m\frac{P_{T_b}}{P_b})^{m+k}}{(m+k)\Gamma(m)} r^{\alpha m+\alpha k+1}, 0 < r < R \quad (5)$$

Using the Mapping theorem [10] and following an approach similar to that in [19], it can be shown that a 1-D PPP with an intensity function $\bar{\lambda}$ and a path-loss exponent α is equivalent (in terms of the aggregate interference statistics at the PR) to a 1-D PPP with a unit path-loss exponent and an intensity function of $\tilde{\lambda}$ where

$$\tilde{\lambda} = \frac{2\pi\lambda}{\alpha} \sum_{k=0}^{\infty} \frac{(-1)^k}{k!} \frac{(m\frac{P_{T_b}}{P_b})^{m+k}}{(m+k)\Gamma(m)} r^{m+k+\frac{2}{\alpha}-1}, 0 < r < R^{\alpha}. \quad (6)$$

With the new intensity function $\tilde{\lambda}$, the interference from the i-th transmitting secondary node becomes $I_i = P_{CR}|h_i|^2 r^{-1}$.

B. Derivation of the MGF

We will now derive the MGF using the results obtained in the previous subsection. The MGF of I is defined by $M_I(s) = E[e^{-sI}]$. Using the Campbell's theorem [10], $E[e^{-sI}]$ is written as

$$E[e^{-sI}] = e^{\left(\int_0^{R^{\alpha}} E_{|h_i|^2}\left[e^{-sP_{CR}|h_i|^2 r^{-1}} - 1\right]\tilde{\lambda} dr\right)}. \quad (7)$$

Performing the expectation with respect to $|h_i|^2$ using (2) results in

$$E[e^{-sI}] = e^{\left(\int_0^{R^{\alpha}} \left[\frac{1}{(1+s\frac{P_{CR}}{rm})^m} - 1\right]\tilde{\lambda} dr\right)}. \quad (8)$$

After substituting (6) for $\tilde{\lambda}$ and performing the integration, $M_I(s)$ is given by (11).

C. Random transmit powers

The previous analysis assumed the transmit power of the secondary nodes to be constant and identical. However, to model a more practical scenario, we assume the transmit power varies between 0 and a maximum allowed power P_{max} with $M+1$ different discrete power levels. Then, the transmit power of the l-th level would become $\frac{l}{M}P_{max}$, where $l = 0 \ldots M$, and would have a probability of p_l. $\sum_{l=0}^{M} p_l = 1$, and this probability distribution depends on power controlling algorithms, nature of the device, and the area geography. Communication systems such as GSM and IS-95 have power controlling schemes based on discrete power levels [20]. Incorporating random power levels to (7) gives us

$$E[e^{-sI}] = e^{\left(\int_0^{R^{\alpha}} E_{|h_i|^2}\left[\sum_{l=0}^{M} p_l e^{-s\frac{l}{M}P_{max}|h_i|^2 r^{-1}} - 1\right]\tilde{\lambda} dr\right)}$$
$$= e^{\left(\int_0^{R^{\alpha}} \left[\sum_{l=0}^{M} \frac{p_l}{(1+s\frac{lP_{max}}{rmM})^m} - 1\right]\tilde{\lambda} dr\right)}. \quad (9)$$

Finally, when the integration with respect to $\tilde{\lambda}$ is performed, we obtain equation (12) for $M_I(s)$ with random transmit powers.

D. Average interference

An important performance measure is the average interference ($E[I]$). From the Campbell's theorem, $E[I]$ is derived as

$$E[I] = \int_0^{R^{\alpha}} E_{|h_i|^2}[P_{CR}|h_i|^2 r^{-1}]\tilde{\lambda}\, dr$$
$$= 2\pi\lambda P_{CR} \sum_{k=0}^{\infty} \frac{(-1)^k}{k!} \frac{(m\frac{P_{T_b}}{P_b})^{m+k}}{(m+k)\Gamma(m)} \frac{R^{\alpha m+\alpha k-\alpha+2}}{\alpha m+\alpha k-\alpha+2}. \quad (10)$$

Replacing P_{CR} in (10) with $\sum_{l=0}^{M} p_l \frac{l}{M} P_{max}$ gives the average interference when the transmit powers are random.

IV. Outage Probability

We will now derive the outage probability of the PR using the results for the aggregate interference MGF obtained earlier.

Let the transmit power level of the primary transmitter be P_p, and the distance between the primary transmitter and PR be R_{pr}. The SINR of the PR (γ) is written as $\gamma = \frac{P_p R_{pr}^{-\alpha}|h|^2}{I+\sigma_n^2}$, where $P_p R_{pr}^{-\alpha}|h|^2$ is the received primary signal power at the PR. σ_n^2 and $|h|^2$ respectively denote the noise variance and the channel gain distributed according to (2). The CDF of the SINR is obtained as (see Appendix I for proof)

$$F_{\gamma}(x) = 1 - e^{-\frac{mx\sigma_n^2}{P_p R_{pr}^{-\alpha}}} \sum_{\nu=0}^{m-1} \frac{1}{\nu!} \left(\frac{mx}{P_p R_{pr}^{-\alpha}}\right)^{\nu}$$
$$\times \sum_{\mu=0}^{\nu} \binom{\nu}{\mu} (\sigma_n^2)^{\nu-\mu} (-1)^{\mu} M_I^{(\mu)}\left(s|_{s=\frac{mx}{P_p R_{pr}^{-\alpha}}}\right) \quad (13)$$

We will see in Section V that the infinite sum for $M_I(s)$ (11) used in (13) converges in a finite amount of terms. Substitution of the required threshold for proper reception (γ_{th}) instead of x gives us the outage.

$$M_I(s) = e^{\left[2\pi\lambda\sum_{k=0}^{\infty}\frac{(-1)^k}{k!}\frac{(m\frac{P_{T_b}}{P_b})^{m+k}}{(m+k)\Gamma(m)}\left(\frac{R^{2\alpha m+\alpha k+2}}{2\alpha m+\alpha k+2}\left(\frac{m}{sP_{CR}}\right)^m\ {}_2\mathcal{F}_1\left(m,k+2(m+\frac{1}{\alpha});1+k+2(m+\frac{1}{\alpha});-\frac{mR^{\alpha}}{sP_{CR}}\right)-\frac{R^{\alpha m+\alpha k+2}}{\alpha m+\alpha k+2}\right)\right]} \tag{11}$$

$$M_I(s) = e^{\left[2\pi\lambda\sum_{k=0}^{\infty}\frac{(-1)^k}{k!}\frac{(m\frac{P_{T_b}}{P_b})^{m+k}}{(m+k)\Gamma(m)}\left(\sum_{l=0}^{M}p_l\frac{R^{2\alpha m+\alpha k+2}}{2\alpha m+\alpha k+2}\left(\frac{mM}{slP_{max}}\right)^m\ {}_2\mathcal{F}_1\left(m,k+2(m+\frac{1}{\alpha});1+k+2(m+\frac{1}{\alpha});-\frac{mMR^{\alpha}}{slP_{max}}\right)-\frac{R^{\alpha m+\alpha k+2}}{\alpha m+\alpha k+2}\right)\right]} \tag{12}$$

V. Numerical Results

This section will provide numerical results on the PR's outage probability, mean aggregate interference power and the viability of approximating the sum of (4) with the first term ($k = 0$ only). For consistence, we will use the parameters $R = 100$, $R_{pr} = 30$, $\lambda = 1 \times 10^{-3}$, $\gamma_{th} = 1$. Furthermore, we will keep $\sigma_n^2 = 0$ in order to highlight the interference. For brevity, we will only consider constant secondary node transmit powers.

Figure (2) validates the theoretical results by plotting the PR outage probability as a function of the primary transmit power level P_p. The theoretical plots use only 20 summations (From (13) and (11)). As the m increases (fading severity reduces), we observe a lower outage probability. This may appear counter intuitive because the interfering signals are not significantly faded with an increased m. However, the primary factor concerning interference is the beacon misdetection. With higher m, the beacon is detected more, and the secondary nodes refrain from transmitting concurrently with the primary users. With higher P_p, the slope of the curves (diversity order) changes with respect to m.

The mean aggregate interference is plotted in Figure (3) with respect to the fading severity (m) for different path-loss exponent values (α). As expected, the mean interference drops with respect to m. However, the rate of this change is different for various path-loss exponents. The mean aggregate interference drops at a greater rate when α is lower. This is due to the reduction in misdetection.

The exact MGF of the aggregate interference is provided in (11) using (4), but contains an infinite series. Although this series quickly converges, having a simpler result containing only a single term would be ideal. Figure (4) shows occasions when the approximation of replacing the infinite sum of (4) with the first term is valid. For a lower beacon reception threshold to beacon transmit power ratio ($\frac{P_{T_b}}{P_b} = 2 \times 10^{-7}$) and $m = 1$, the approximation with only 1 term of the sum is almost identical with that of the exact sum (Note that the curves overlap in the graph). When both m and $\frac{P_{T_b}}{P_b}$ increases, the curves diverge, indicating that several terms of the sum need to be considered for an accurate result. As a side-note, when $m = 2$, the outage experiences a 20 dB reduction when the beacon reception threshold to beacon transmit power ratio drops by tenfold.

VI. Conclusion

This paper analyzed the aggregate interference from inter-weave secondary nodes spatially distributed over a finite area with either constant or random transmit powers. Nakagami-m fading and path loss were incorporated. The exact MGF and mean of the aggregate interference was derived along with the PR outage probability. Furthermore, we provided a simpler approximation to the exact MGF which is accurate under lower Nakagami-m parameters and beacon reception threshold to beacon transmit power ratios. We conclude that a higher m parameter (lower fading severity) provides a

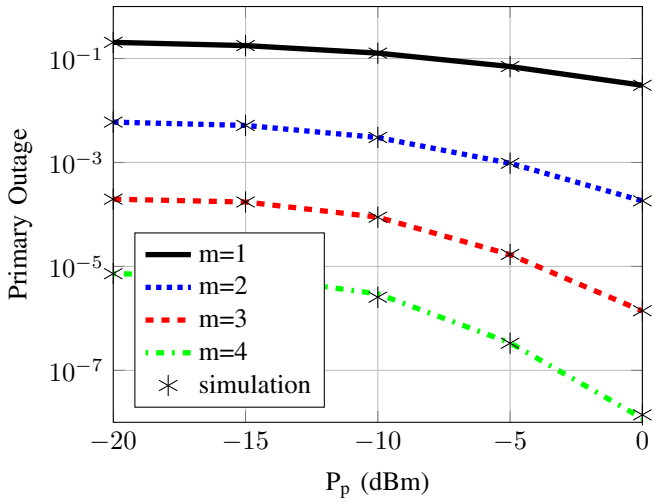

Fig. 2: The PR outage probability vs the primary power level P_p for different fading severities. $\alpha = 3$, $P_{CR} = 4$ dBm, and $\frac{P_{T_b}}{P_b} = 2 \times 10^{-8}$.

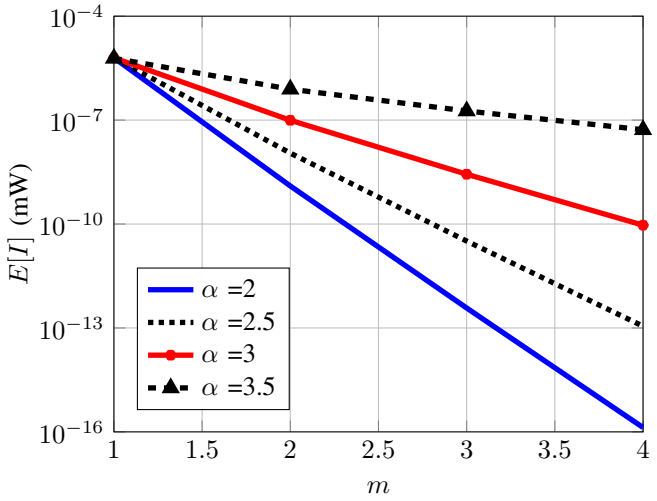

Fig. 3: The mean aggregate interference vs the fading severity (m) under different α. $P_{CR} = 10$ dBm, and $\frac{P_{T_b}}{P_b} = 2 \times 10^{-8}$.

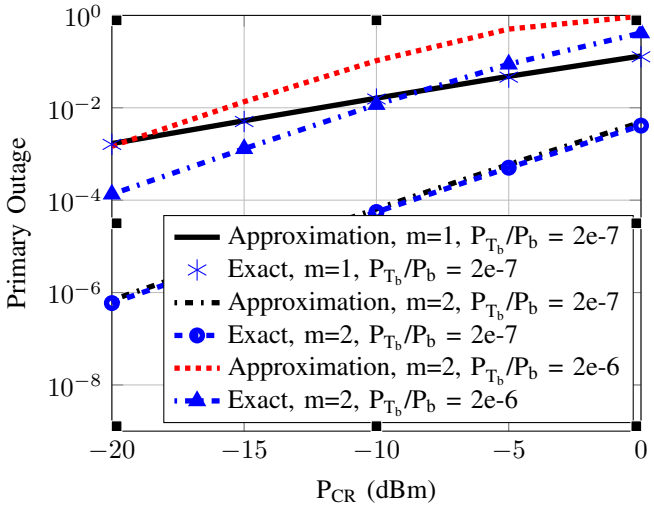

Fig. 4: The PR outage probability vs secondary node power level P_{CR}, for the exact sum of (11) and the approximation with only the first term. $\alpha = 3$, and $P_p = 5\,\text{dBm}$.

favorable environment due to improved accuracy of beacon detection. As well, the mean aggregate interference (in dB) shows a linear relationship vs m when m is higher with the gradient depending on the path loss exponent. Moreover, a 10 dB decrease in the beacon reception threshold to beacon transmit power ratio provides almost a 20 dB reduction in outage highlighting its importance in avoiding interference.

Appendix I :Proof of CDF $F_\gamma(x)$

The CDF of the outage $F_\gamma(x) = \Pr[\gamma \leq x]$. Therefore, after substituting for γ, and using equation (2),

$$F_{\gamma/I}(x)=\Pr\left[|h|^2\leq\frac{x(I+\sigma_n^2)}{P_pR_{pr}^{-\alpha}}\right]=1-\frac{\Gamma\left(m,m\frac{x(I+\sigma_n^2)}{P_pR_{pr}^{-\alpha}}\right)}{\Gamma(m)}. \quad (14)$$

Expanding (14) gives us

$$F_\gamma(x)=1-E_I\left[\int_{\frac{x(I+\sigma_n^2)}{P_pR_{pr}^{-\alpha}}}^{\infty}\frac{m^m}{\Gamma(m)}x^{m-1}e^{-mx}dx\right]. \quad (15)$$

By substituting $y = mx$ for integer m, we can write

$$\begin{aligned}
F_\gamma(x)&=1-E_I\left[\frac{1}{\Gamma(m)}\int_{\frac{mx(I+\sigma_n^2)}{P_pR_{pr}^{-\alpha}}}^{\infty}y^{m-1}e^{-y}dy\right]\\
&=1-E_I\left[e^{-\frac{mx(I+\sigma_n^2)}{P_pR_{pr}^{-\alpha}}}\sum_{\nu=0}^{m-1}\frac{1}{\nu!}\left(\frac{mx(I+\sigma_n^2)}{P_pR_{pr}^{-\alpha}}\right)^{\nu}\right]\\
&=1-e^{-\frac{mx\sigma_n^2}{P_pR_{pr}^{-\alpha}}}\sum_{\nu=0}^{m-1}\frac{1}{\nu!}\left(\frac{mx}{P_pR_{pr}^{-\alpha}}\right)^{\nu}\\
&\times\sum_{\mu=0}^{\nu}\binom{\nu}{\mu}(\sigma_n^2)^{\nu-\mu}E_I\left[I^\mu e^{-\frac{mxI}{P_pR_{pr}^{-\alpha}}}\right]\\
&=1-e^{-\frac{mx\sigma_n^2}{P_pR_{pr}^{-\alpha}}}\sum_{\nu=0}^{m-1}\frac{1}{\nu!}\left(\frac{mx}{P_pR_{pr}^{-\alpha}}\right)^{\nu}\\
&\times\sum_{\mu=0}^{\nu}\binom{\nu}{\mu}(\sigma_n^2)^{\nu-\mu}(-1)^\mu M_I^{(\mu)}\left(s|_{s=\frac{mx}{P_pR_{pr}^{-\alpha}}}\right),
\end{aligned}$$

which is equation (13).

However, because CR systems are primarily inhibited by interference, the noise can be neglected. If so, $F_\gamma(x)$ becomes

$$F_\gamma(x)=1-\sum_{\nu=0}^{m-1}\frac{(-1)^\nu}{\nu!}\left(\frac{mx}{P_pR_{pr}^{-\alpha}}\right)^{\nu}M_I^{(\nu)}\left(s|_{s=\frac{mx}{P_pR_{pr}^{-\alpha}}}\right). \quad (16)$$

References

[1] I. F. Akyildiz, W.-Y. Lee, M. C. Vuran, and S. Mohanty, "Next generation/dynamic spectrum access/cognitive radio wireless networks: A survey," *Computer Networks*, vol. 50, no. 13, pp. 2127–2159, 2006. [Online]. Available: http://www.sciencedirect.com/science/article/pii/S1389128606001009

[2] M. Derakhshani and T. Le-Ngoc, "Aggregate interference and capacity-outage analysis in a cognitive radio network," *IEEE Trans. Veh. Technol.*, vol. 61, no. 1, pp. 196–207, Jan. 2012.

[3] M. Sherman, A. Mody, R. Martinez, C. Rodriguez, and R. Reddy, "IEEE standards supporting cognitive radio and networks, dynamic spectrum access, and coexistence," *IEEE Commun. Magazine*, vol. 46, no. 7, pp. 72–79, Jul. 2008.

[4] C.-H. Lee and M. Haenggi, "Interference and outage in poisson cognitive networks," *IEEE Trans. Wireless Commun.*, vol. 11, no. 4, pp. 1392–1401, Apr. 2012.

[5] A. Babaei and B. Jabbari, "Interference modeling and avoidance in spectrum underlay cognitive wireless networks," in *Proc. IEEE ICC*, May 2010, pp. 1–5.

[6] X. Song, C. Yin, D. Liu, and R. Zhang, "Spatial opportunity in cognitive radio networks with threshold-based opportunistic spectrum access," in *Proc. IEEE ICC 2013*, 2013, pp. 2695–2700.

[7] M. Vu, N. Devroye, and V. Tarokh, "On the primary exclusive region of cognitive networks," *IEEE Trans. Wireless Commun.*, vol. 8, no. 7, pp. 3380–3385, Jul. 2009.

[8] A. Rabbachin, T. Q. S. Quek, H. Shin, and M. Z. Win, "Cognitive network interference," *IEEE J. Sel. Areas Commun.*, vol. 29, no. 2, pp. 480–493, Feb. 2011.

[9] S. Kusaladharma and C. Tellambura, "Impact of beacon misdetection on aggregate interference for hybrid underlay-interweave networks," *IEEE. Commun. Lett.*, vol. 17, no. 11, pp. 2052–2055, 2013.

[10] J. F. Kingman, *Poisson Processes*. Oxford University Press, 1993.

[11] Z. Chen, C.-X. Wang, X. Hong, J. Thompson, S. Vorobyov, X. Ge, H. Xiao, and F. Zhao, "Aggregate interference modeling in cognitive radio networks with power and contention control," *IEEE Trans. Commun.*, vol. 60, no. 2, pp. 456–468, Feb. 2012.

[12] S. Kusaladharma and C. Tellambura, "Aggregate interference analysis for underlay cognitive radio networks," *IEEE Wireless Commun. Lett.*, vol. 1, no. 6, pp. 641–644, 2012.

[13] M. Haenggi, *Stochastic Geometry for Wireless Networks*. Cambridge University Press, 2012.

[14] A. Goldsmith, *Wireless Communications*. Cambridge University Press, 2005.

[15] I. Gradshteyn and I. Ryzhik, *Table of integrals, Series, and Products*, 7th ed. Academic Press, 2007.

[16] D. Stoyan, W. S. Stoyan, Kendall, and J. Mecke, *Stochastic Geometry and it's Applications*. John Wiley & Sons Ltd., 1995.

[17] A. Molisch, *Wireless Communications*. Wiley-IEEE Press, 2011.

[18] S. Atapattu, C. Tellambura, and H. Jiang, "A mixture gamma distribution to model the SNR of wireless channels," *IEEE Trans. Wireless Commun.*, vol. 10, no. 12, pp. 4193–4203, Dec. 2011.

[19] P. Madhusudhanan, J. G. Restrepo, Y. Liu, T. X. Brown, and K. Baker, "Downlink performance analysis for a generalized shotgun cellular system," *CoRR, 2010. [Online]. Available: http://arxiv.org/abs/1002.3943*.

[20] Y. Xing and R. Chandramouli, "Distributed discrete power control for bursty transmissions over wireless data networks," in *Proc. IEEE ICC*, vol. 1, June 2004, pp. 139–143 Vol.1.